Size Effects in Unreinforced and Lightly Reinforced Concrete Beams Failing in Flexure

Levingshan Augusthus Nelson

School of Science, Engineering and Environment, University of Salford, United Kingdom

Janet M. Lees

Department of Engineering, University of Cambridge, United Kingdom

Laurence Weekes

School of Science, Engineering and Environment, University of Salford, United Kingdom

Abstract

Fracture-based models commonly use a characteristic length as the basis for determining size effects in concrete beams. The characteristic length is related to the concrete fracture process zone and defined in terms of the concrete fracture properties. Semi-empirical constants are then developed to accommodate any unidentified (geometric or crack bridging) parameters. However, a reliance on semi-empirical factors can limit the applicability to different systems, concretes and reinforcing materials. The aim of the current work is to formulate an analytical size effect model based solely on fundamental material and geometric properties. The particular focus is unreinforced and lightly reinforced concrete beams that fail in flexure due to unstable crack propagation. The proposed 'generalised' characteristic length approach is based on the mode-I fracture behaviour of concrete and includes crack bridging forces due to the presence of longitudinal reinforcement. The theoretical expressions suggest that the geometric shape of a beam, the fracture properties of the concrete and the crack bridging forces (where present) significantly influence the characteristic length. Experimental investigations on geometrically similar unreinforced and lightly reinforced concrete beams in 2-D are undertaken as a means for initial validation. The validation is then extended to a wider dataset of existing experimental results in the literature. The generalised characteristic length approach is able to capture both the influence of the concrete strength and the size effect mitigation due to the inclusion of longitudinal reinforcement. This confirms that the generalised approach holds promise and could be expanded to other quasi-brittle materials and non-conventional reinforcing materials.

Keywords: characteristic length; size effect; reinforced concrete; fracture mechanics

---

Nomenclature

a	Crack depth
B	Dimensionless constant
b	Width of concrete beam
c	Concrete cover
D	Depth of the plate/beam
D_0	Characteristic length
d_a	Maximum aggregate size
E	Elastic modulus of concrete
E_f	Elastic modulus of reinforcement
f_c	Concrete compressive cube strength
f_{cy}	Concrete compressive cylinder strength
f_f	Yield stress of reinforcement
F_s	Crack bridging force applied by reinforcement
f_t	Tensile strength of concrete
G_F	Concrete fracture toughness

$k\left(\frac{a}{D}\right)$	Shape factor
K_I	Stress intensity
K_{Ic}	Critical stress intensity
K_{IF}	Stress intensity factor due to the crack bridging force in the reinforcement
K_{IM}	Stress intensity factor due to bending
M	Bending moment across a crack
n	Exponential power of normal stress distribution in the fracture process zone
s	Shear span of concrete beam
$\frac{s}{d}$	Shear span to depth ratio
Δa	Additional crack extension
Δa_e	Depth of fracture process zone
Δ_{Nu}	Norminal strength
η	Geometric shape constant
λ	Size effect reduction factor
ψ	Portion of reinforcement yield force
ρ	Percentage of reinforcement
σ	Tensile stress perpendicular to crack face
σ_c	Concrete plastic strength
σ_n	Uniform tensile stress away from crack
CMOD	Crack mouth opening displacement
LEFM	Linear ealstic fracture mechanics
$2-D$	Two dimensionsional

1. Introduction

It has been observed that structural concrete exhibits a strong size effect. Researchers initially believed that size effects were associated with the variability in the concrete material strength (statistical size effect) [1]. However, it has since been discovered that size effects depend on the material, mechanical and geometrical properties of concrete [2]. Bazant's earlier work on size effect resulted in a size effect law, which was for quasi-brittle materials with a pre-existing crack or crack notch. This was later classified as the Type 2 deterministic (or energetic) size effect problem [2, 3]. It was shown that quasi-brittle materials without a pre-existing crack or crack notch manifest both statistical and deterministic size effects; thus Weibull and Bazant's models were integrated to address what was classified as the Type 1 size effect problem [4, 5, 6]. Size effects that can influence the nominal strength of concrete structures include a boundary layer effect, a fracture mechanics size effect, an influence due to the fractal nature of the crack surface, variability in the material strength, and a size effect associated with chemical reactions, heat conduction and pore water transfer [7]. The contribution of each of these factors is not fully understood.

The mechanical behaviour of concrete is a result of multiple mechanisms at macro-, meso- and micro- length scales. Recently, the modelling of concrete at the meso-length scale has been a focal point. At the meso-scale, concrete is taken as a multi-phase composite material with the mortar, the aggregates, and the interfaces between the mortar and aggregates taken as separate phases [8]. The material size effects are then investigated [9, 10, 11] albeit that typically the primary distortion/deformation is limited to the interface elements between the mortar and aggregates. The purpose of this paper is to investigate the size effects at the system level (macro-length scale) with the inclusion of crack bridging effects.

The properties that determine the Type 2 size effect can be expressed in terms of an intrinsic or characteristic length which is defined by linear or non-linear fracture mechanics. Size effects in flexural unreinforced concrete beams that fail due to a single crack have been studied extensively [12, 13, 14]. For longitudinally reinforced concrete beams that fail in flexure due to unstable crack propagation (where the post peak loads do not exceed the peak load, which corresponds to the load at crack initiation), the size effects will depend on the percentage of reinforcement. Ruiz et al [15] and Carpinteri et al [16] showed that lightly reinforced concrete beams may not develop a full or partial hinge, and thus exhibit a size effect. Gerstle et al [17] used a cohesive crack model to theoretically investigate the flexural behaviour of longitudinally reinforced concrete beams and observed a strong size effect in a beam with less than 0.1% of longitudinal reinforcement. With increasing percentages of longitudinal reinforcement size effects were reduced. Based on Hillerborg's [18] study of Corley's experimental results [19] size effects were found to be less significant for a beam with more than 1% of longitudinal reinforcement. It has been shown that over-reinforced concrete beams exhibit size effects in flexure as a result of concrete crushing in the compression zone [20, 21]. Concrete crushing in the compression zone is the leading cause of failure when an over-reinforced concrete beam fails due to a diagonal shear-compression failure, where a similar size effect phenomenon was observed [22, 23]. However, size effects due to concrete crushing are beyond the scope of this paper; thus, discussed no further.

In practice beams typically contain more than the minimum amount of longitudinal reinforcement and so are not as susceptible to flexural size effects. Hence, size effects in lightly reinforced beams that fail due to mode I fracture have not been widely studied. In contrast, size effects in longitudinally reinforced concrete beams that fail in shear [24, 25, 26] have been the subject of significant research effort. Statistical analyses of existing experimental results [27] have then been used as the basis for the development of semi-empirical models. These semi-empirical models are typically based solely on the concrete material properties (e.g. Bažant and Kim [27]). Numerical analyses, e.g. Gustafsson and Hillerborg [28] also suggest that the characteristic length is a material property of concrete. For concrete beams with internal longitudinal and transverse shear reinforcement, Bažant and Sun [29] proposed an approach which takes into account transverse steel in the sense of being a systems property.

The semi-empirical nature of some of the proposed models and the lack of a unifying theory means that it is difficult to extend existing research to consider new types of concretes and/or other reinforcing materials. Furthermore, the transition from brittle to ductile behaviour is not depicted within a common framework. To address these shortcomings, a new characteristic length, hereafter referred to as the 'generalised characteristic length', was derived from first principles using a mode I non-linear fracture model together with a crack bridging effect from the reinforcement. The uniqueness of the generalised characteristic length is that the concrete element, which exhibits size effects, is contemplated as a system property (a combination of material, geometry and interaction properties). This is in contrast to existing size effect models that consider the concrete element as a material property alone. Moreover, the resulting expression for the generalised characteristic length is defined in terms of fundamental contributing factors such as the geometry of a beam, material properties of the concrete, and crack bridging force. Each of these contributions provides insight into how the predicted characteristic lengths, and hence size effects, depend on prescribed parameters such as the concrete strength and reinforcement percentage. Geometrically similar unreinforced and lightly reinforced concrete beams are tested to supplement a validation database against which the model predictions are interrogated.

2. Fracture mechanics - size effects

Linear elastic fracture mechanics (LEFM) can be used to describe crack propagation in brittle materials, where the fracture process zone is negligible [30]. However, quasi-brittle materials such as concrete, ceramics and hardened ice deviate from LEFM behaviour as a result of a sizeable fracture process zone at the crack tip compared to the size of specimen. In order to minimise the level of additional complexity due to the non-linear behaviour, various modified

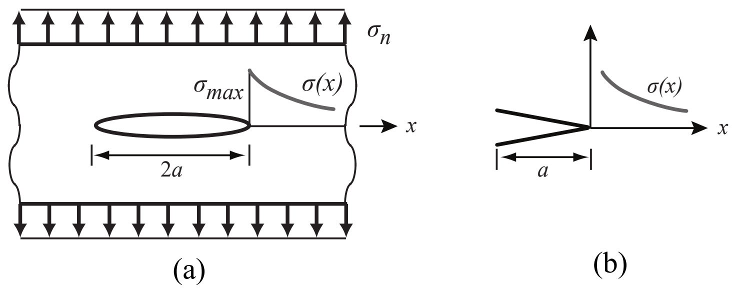

Figure 1: Distribution of internal stress in the region of a flaw: (a) elliptical flaw and (b) sharp flaw.

LEFM models have been proposed.

2.1. LEFM

In LEFM, it is assumed that a crack propagates when the applied stress intensity (or the resultant stress intensity if there is more than one external load) reaches the material critical stress intensity factor. In terms of an energy approach, this is analogous to the energy available for crack propagation reaching the material fracture toughness. Fig. 1 illustrates the assumed mode I fracture conditions in a semi-infinite $2-D$ plate subjected to a uniform tensile stress, σ_n. For an infinitely wide plate with a crack length of $2a$, the stress concentration at the crack tip is defined in terms of the applied stress (σ_n). The associated value of the mode I fracture stress intensity factor is given by Irwin [31] as:

$$K_I = \sigma_n \sqrt{a} k \left(\frac{a}{D} \right) \tag{1}$$

where D is the overall depth of the plate, a is the crack depth and $k\left(\frac{a}{D}\right)$ is a factor, also known as the shape factor, which is dependent on the depth of the crack and geometry of the structure. At failure, the stress intensity K_I would equal the fracture toughness or critical stress intensity factor, K_{Ic} of the material.

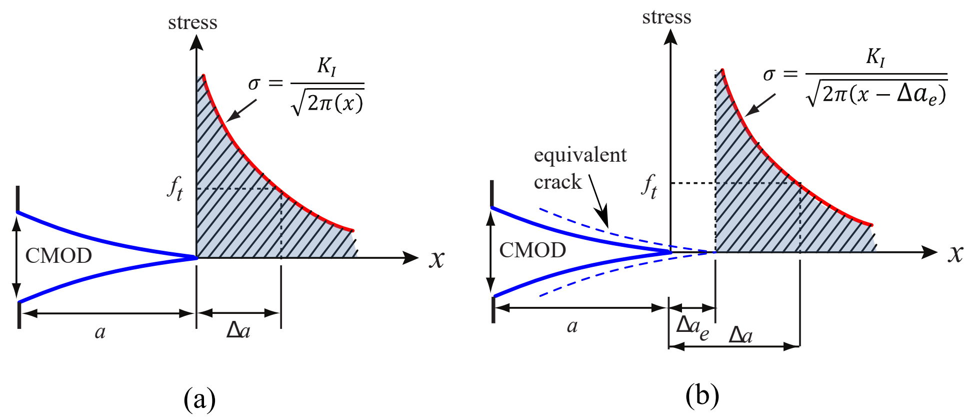

Figure 2: An (a) LEFM and (b) equivalent crack model approximation.

2.2. Equivalent crack model

The LEFM approach assumes that the inelastic fracture process zone is zero (see Fig. 2(a)). In practice the fracture process zone in concrete has a finite size since the material is quasi-brittle. It has been shown that the departure between actual and theoretical predictions using LEFM in large concrete structures such as dams, where the size of the fracture process zone is much smaller than the size of the structure, is minimal [32]. Thus, the prediction of size effect in a large concrete structure using LEFM can be acceptable. Nonetheless, when it is necessary to take into account the fracture process zone, equivalent crack models have been proposed [33]. Equivalent crack models are based on the concept that the non-linear fracture process zone decreases the stiffness of the structure thereby allowing the crack length to increase while the rest of the structure continues to behave as a linear elastic material [34, 35]. The equivalent crack model therefore simulates the response of the specimen and the fracture process zone by assuming that the crack tip is ahead of the actual crack tip. Fig. 2(b) shows an equivalent crack model which includes the fracture process zone (the zone with micro cracks). In the figure, f_t is the tensile strength of the concrete, CMOD is the crack mouth opening displacement, a is the crack depth, Δa_e is the fracture process zone where the stress reaches infinity and Δa is the additional crack extension to the point where the tensile strength of concrete is reached. In the equivalent crack model, the effective crack length is implicitly taken as $(a + \Delta a_e)$ and the rest of the specimen is linear elastic. Elices and Planas [36] studied tension softening models to define the equivalence between a specimen with an equivalent crack and a linear elastic cracked specimen. It was found that the equivalent crack solution approaches that of the LEFM model as the size of the fracture process zone reduces.

2.3. Bazant's size effect model

Bazant's size effect equation for pure tension mode I fracture using an equivalent elastic crack model is summarised in this section. For further details, please see [3]. Using an equivalent crack approach the effective crack depth is modelled as the addition of the actual crack depth (a) and a fracture process zone in the region ahead of the original crack tip Δa_e (see Fig. 2(b)), at the point of crack propagation. Therefore, for a quasi-brittle material, Irwin's stress intensity factor can be rewritten as:

$$K_{Ic} = \sigma_{Nu}\sqrt{D}k\left(\frac{a+\Delta a_e}{D}\right) \tag{2}$$

where K_{Ic} is the critical stress intensity factor and σ_{Nu} is the nominal strength. Using this substitution, and approximating $k^2\left(\frac{a}{D}+\frac{\Delta a_e}{D}\right)$ using the first two terms of a Taylor series expansion with respect to $\frac{a}{D}$, gives:

$$k^2\left(\frac{a}{D}+\frac{\Delta a_e}{D}\right) \approx k^2\left(\frac{a}{D}\right) + 2k\left(\frac{a}{D}\right)k'\left(\frac{a}{D}\right)\frac{\Delta a_e}{D} \tag{3}$$

where

$$k'\left(\frac{a}{D}\right) = \frac{\partial k\left(\frac{a}{D}\right)}{\partial\left(\frac{a}{D}\right)} \tag{4}$$

By defining

$$B = \frac{K_{Ic}}{f_t\sqrt{2k\left(\frac{a}{D}\right)k'\left(\frac{a}{D}\right)\Delta a_e}} \tag{5}$$

and

$$D_0 = \frac{2k'\left(\frac{a}{D}\right)\Delta a_e}{k\left(\frac{a}{D}\right)} \tag{6}$$

Eqn. 2 can be simplified to

$$\sigma_{Nu} = \frac{Bf_t}{\sqrt{1 + \frac{D}{D_0}}} \tag{7}$$

where f_t is the tensile strength of the material, B is a dimensionless constant, D_0 has a dimension of length and is known as the characteristic length, and D is a characteristic dimension, which in the current work is taken as the beam depth. Both B and D_0 depend on the fracture properties of the material and the geometry of the structure, but are not dependent on the depth or characteristic size of the structure, as will be discussed later. Eqn. 7 is also known as Bazant's size effect law.

2.4. Fracture and ultimate nominal strength

A graphical representation of Eqn. 7 is shown schematically as the curved line in Fig. 3 where the relationship between the nominal strength σ_{Nu} and the characteristic size D of a beam has been plotted. In Fig. 3, the plastic strength and the linear elastic fracture mechanics failure criterion are shown as a horizontal line and an inclined line with a 1:2 slope respectively. Small structures do not show a significant strength reduction. Therefore, in this case the nominal strength approaches Bf_t, where $Bf_t (= \sigma_c)$ is the plastic strength. A size effect reduction factor $\lambda \left(= \frac{\sigma_{Nu}}{\sigma_c}\right)$ relative to the nominal plastic strength can then be defined as

$$\lambda = \frac{1}{\sqrt{1 + \frac{D}{D_0}}} \tag{8}$$

In practical applications, the majority of design codes are based on lower bound plasticity analyses [37, 38]. Plasticity theory has no size effects. Nevertheless, since plasticity equations are available in design codes, the incorporation

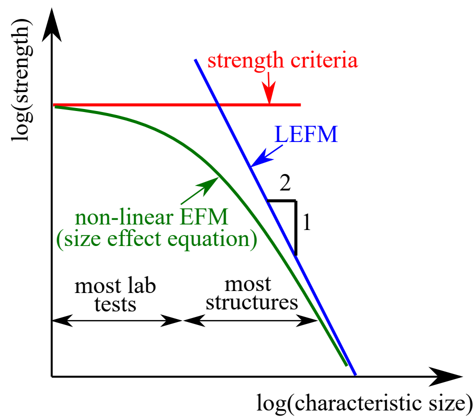

Figure 3: Relationship between strengths and characteristic size

of a size effect reduction factor such as that given by Eqn. 8 into a plastic approach has been seen as preferable to developing a new analytical expression.

3. Derivation of generalised characteristic length

Bazant's size effect equation, developed by combining linear elastic fracture mechanics and the equivalent crack model, shows that the characteristic length D_0 plays an important role in defining the size effect in concrete beams. However, the presence of reinforcement would be expected to change the characteristic length and, to date, this issue has not been sufficiently addressed. In the following, a new, 'generalised', characteristic length is derived using an approach that is equally applicable to beams with, or without, reinforcement.

The generalised characteristic length is derived by combining a non-linear fracture mechanics model and crack bridging forces to represent longitudinal reinforcement.

To reflect the additional crack bridging forces due to the presence of reinforcement, the principle of the superposition of stress intensity factors is used. In linear elastic fracture mechanics (LEFM), the mode I stress intensity factors for various combinations of external loading can be superposed [16][39]. Therefore, Bosco and Carpinteri [40] proposed that the resultant stress intensity factor for

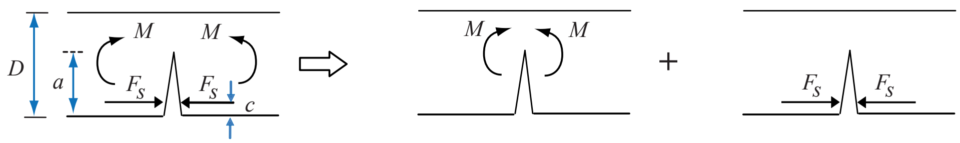

Figure 4: Superposition of external applied loads.

a concrete beam with longitudinal reinforcement subjected to bending can be calculated as the superposition of the stress intensity factor due to the applied bending moment and the stress intensity factor due to the force in the reinforcement. This superposition is shown schematically in Fig. 4. Using this concept the resultant critical stress intensity factor at the onset of crack propagation for a given crack depth, a, can be given as

$$K_{Ic} = K_{IM} + K_{IF} \tag{9}$$

where K_{IM} and K_{IF} are the stress intensity factors due to the bending moment (M) and the reinforcement forces, F_s, respectively. When reinforcement bridges a crack, the resultant stress at the crack tip is enhanced by the contribution from K_{IF}. The stress and the length of the non-linear zone therefore change. A representation of a crack region with reinforcement bridging the crack using an equivalent crack model combined with LEFM is shown in Fig. 5. The contribution from the reinforcement is represented as equal and opposite forces F_s at the crack face.

At the crack tip, the crack has already completely softened and the points ahead of the crack tip are in an intermediate state of fracture. Therefore, the stress distribution in the non-linear elastic zone can be taken as a polynomial function $\left(\sigma = f_t \left(\frac{x}{\Delta a}\right)^n\right)$ [41]. The stress resultant from an inelastic zone of size Δa can be set equal to the stress resultant of the elastically calculated stress $\left(\sigma = \frac{K_{Ic}+K_{IF}}{\sqrt{2\pi(x-\Delta a_e)}}\right)$. Due to the equivalent crack model assumption, the far field stress is taken from LEFM. Therefore, the area under the plastic stress field is equal to that of the elastic stress field. Thus, in Fig. 5 the area of the

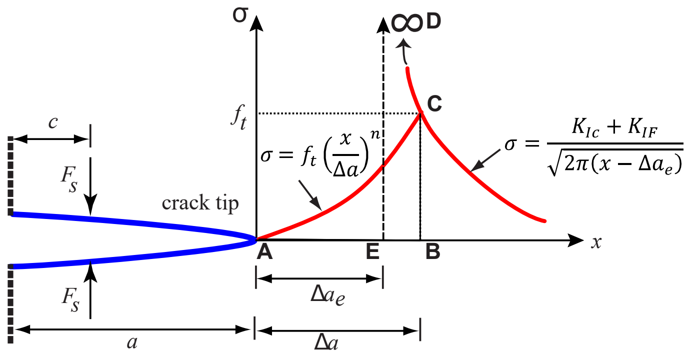

Figure 5: Stress distribution at the crack tip with a crack bridging force in the reinforcement

region AEBCA must be equal to the area of region EBCDE. Therefore,

$$\int_{\Delta a_e}^{\Delta a} \frac{K_{Ic} + K_{IF}}{\sqrt{2\pi(x - \Delta a_e)}} dx = \int_0^{\Delta a} f_t \left(\frac{x}{\Delta a}\right)^n dx \tag{10}$$

Integrating this equation then gives

$$(K_{Ic} + K_{IF}) \sqrt{\frac{2(\Delta a - \Delta a_e)}{\pi}} = \frac{f_t \Delta a}{n+1} \tag{11}$$

The condition $\sigma = f_t$ for $x = \Delta a$, with $\frac{K_{Ic}+K_{IF}}{\sqrt{2\pi(x-\Delta a_e)}}$, immediately leads to

$$\Delta a - \Delta a_e = \frac{1}{2\pi} \left(\frac{K_{Ic} + K_{IF}}{f_t}\right)^2 \tag{12}$$

From Eqn. 11 and 12, the non-linear zone Δa can be calculated as

$$\Delta a = \frac{n+1}{\pi} \left(\frac{K_{Ic}}{f_t}\right)^2 \left(1 + \frac{K_{IF}}{K_{Ic}}\right)^2 \tag{13}$$

By substituting Eqn. 13 into 12, the crack extension can then be given as

$$\Delta a_e = \frac{2n+1}{2\pi} \left(\frac{K_{Ic}}{f_t}\right)^2 \left(1 + \frac{K_{IF}}{K_{Ic}}\right)^2 \tag{14}$$

By comparing Eqn. 14 and 13, it can be seen that the non-linear fracture process length (Δa) and the equivalent crack extension (Δa_e) are proportional. The characteristic length D_0 in Eqn. 7 is also proportional to the equivalent crack extension (Δa_e) (since for a given crack depth $\frac{2k'\left(\frac{a}{D}\right)}{k\left(\frac{a}{D}\right)}$ is a constant). Therefore, it can be represented as

$$D_0 = \eta \frac{2n+1}{2\pi} \left(\frac{K_{Ic}}{f_t}\right)^2 \left(1 + \frac{K_{IF}}{K_{Ic}}\right)^2 \tag{15}$$

where

$$\eta = \frac{2k'_0}{k_0} \tag{16}$$

is a dimensionless geometric constant. The characteristic length D_0 is then the product of four component terms, each of which will influence the characteristic length (from here onwards this will be referred to as the 'generalised' characteristic length). The first term η depends on the geometric shape of the beam. The second term $\frac{2n+1}{2\pi}$ is a function of the concrete stress distribution in the fracture process zone which is reflected in the value of n. The third term, $\left(\frac{K_{Ic}}{f_t}\right)^2$, reflects the concrete material properties, including the tensile strength (f_t) and fracture toughness (K_{Ic}). Finally, $\left(1 + \frac{K_{IF}}{K_{Ic}}\right)^2$ includes both the concrete fracture properties and the crack bridging force(s), which depend on the reinforcement percentage, yield stress and bond-slip behaviour between the concrete and reinforcement.

The generalised characteristic length for mode I flexural cracking from a crack notch in a reinforced bending element was developed from first principles using a non-linear fracture model, known as an equivalent crack model. This non-linear fracture model is applicable to any quasi-brittle material, i.e. concrete, mortar, ceramic and ice. Besides, the crack bridging effect of reinforcement in the non-linear fracture model was implemented as a force. Hence, the crack bridging effect is not limited to steel alone. Therefore, the generalised characteristic length model can be applied to any quasi-brittle materials with any reinforcement that fail due to unstable mode I fracture. However, the main challenges are to establish an accurate shape constant for a given geometry and loading condition and the crack bridging force at the point of crack propagation, which is significantly influenced by the type of reinforcement and the bond-slip behaviour between the quasi-brittle material and the reinforcement. Therefore, a steel-reinforced concrete beam with a crack notch at the mid-span is considered in this investigative section.

With increasing brittleness of concrete, the size of the fracture process zone reduces and so will the generalised characteristic length. Bazant's size effect equation shows that the size effect reduction factor (λ) decreases with a reduction in characteristic length. It can be deduced that the size effect is directly proportional to brittleness. How each parameter in Eqn. 15 is related to brittleness is discussed in more detail in the following.

3.1. Geometric shape constant (η)

The applied bending moment promotes crack propagation whereas the tensile reinforcement resists crack propagation. The nominal strength is calculated based on the applied bending moment. Therefore, the geometric constant is calculated using the shape function associated with the applied bending moment and depends on the loading. For example, the stress intensity factor caused by a bending moment M applied across a cracked section is given in Tada et al. [42] as

$$K_{IM} = \sigma_{Nu}\sqrt{D}k\left(\frac{a}{D}\right) \tag{17}$$

where a is the crack depth, σ_{Nu} is the nominal strength and $k\left(\frac{a}{D}\right)$ is a shape function. For a shear span to depth ratio of 2, the shape function can be given as:

$$k\left(\frac{a}{D}\right) = \sqrt{\frac{a}{D}}\left[\frac{1.99 - \frac{a}{D}\left(1 - \frac{a}{D}\right)\left[2.15 - 3.93\frac{a}{D} + 2.7\left(\frac{a}{D}\right)^2\right]}{\left(1 + \frac{2a}{D}\right)\left(1 - \frac{a}{D}\right)^{\frac{3}{2}}}\right] \tag{18}$$

where the accuracy of the function is within 0.5% for a relative crack depth a/D of up to 0.6. The accuracy reduces for relative crack depths of more than 0.6. For a shear span to depth ratio of 4, the shape function is:

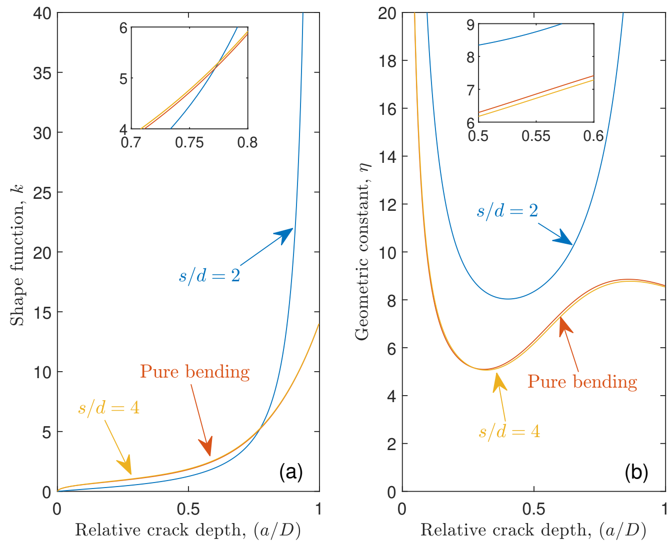

Figure 6: (a) Shape functions and (b) geometric shape constants vs. relative crack depth

$$k\left(\frac{a}{D}\right) = \sqrt{\pi}\left[1.106\left(\frac{a}{D}\right)^{\frac{1}{2}} - 1.552\left(\frac{a}{D}\right)^{\frac{3}{2}} + 7.71\left(\frac{a}{D}\right)^{\frac{5}{2}} - 13.53\left(\frac{a}{D}\right)^{\frac{7}{2}} + 14.23\left(\frac{a}{D}\right)^{\frac{9}{2}}\right] \tag{19}$$

where again an accuracy within 0.5% is expected for a/D of up to 0.6. The shape function for pure bending is:

$$k\left(\frac{a}{D}\right) = \sqrt{\pi}\left[1.122\left(\frac{a}{D}\right)^{\frac{1}{2}} - 1.40\left(\frac{a}{D}\right)^{\frac{3}{2}} + 7.33\left(\frac{a}{D}\right)^{\frac{5}{2}} - 13.08\left(\frac{a}{D}\right)^{\frac{7}{2}} + 14.0\left(\frac{a}{D}\right)^{\frac{9}{2}}\right] \tag{20}$$

and is associated with an accuracy within 0.2% for a relative crack depth of up to 0.6.

In Fig. 6(a), the bending shape functions as a function of relative crack depth for span to depth (s/d) ratios of either 2 or 4 and pure bending are shown. The resulting geometric shape constants η (see Eqn. 16) are plotted against relative crack depth $\left(\frac{a}{D}\right)$ in Fig. 6(b). The shape functions and geometric constants for s/d=4 and pure bending are almost the same but differ from those for s/d=2.

The geometric shape constant is directly proportional to the generalised characteristic length. For a given beam depth, the smallest value of D_0 will result in the largest $\frac{D}{D_0}$ which maximises the denominator in Eqn. 7 leading to the biggest size effect reduction (this represents the smallest size effect reduction factor λ). It should be noted that the highest value of the size effect reduction factor (λ) is 1. For s/d=4 or pure bending, the size effect reduction factor (λ) therefore reaches its minimum value at a relative crack depth of 0.31 (when η reaches a minima of 5.1). For an $\frac{a}{D}$ value between 0.31 and around 0.85, the size effect reduction factor (λ) increases with advancing crack depth. However, for s/d=2, the minimum η value of 8.03 corresponds to a relative crack depth of 0.41. The η value then continues to rise with increasing relative crack depth.

Unreinforced concrete beams fail due to unstable crack growth. Therefore, η should be calculated for the point of the initiation of the crack. For notched beams this would be the tip of the crack notch. Hence, according to the model, the η value will be different for different relative crack notch depths for beams that were otherwise identical. For example, consider two sets of geometrically similar beams with the same shear span to depth ratio of s/d=4 but with relative crack notch depths of 0.3 and 0.5. Based on Fig. 6(b) the beams with relative crack notch depths of 0.3 would exhibit stronger size effects as the η value would be smaller. This demonstrates that the size effect is influenced by the shape of the beam including the crack notch depth.

3.2. Mode I non-linear stress distribution in the fracture process zone (n)

In the generalised formulation, the size effect reduction factor also depends on the exponential power of the stress distribution in the fracture process zone, n which is connected to the material plasticity [7]. Possible stress distributions for different values of n are shown in Fig. 7. Irwin [31] considered a linear stress distribution in the fracture process zone which would be equivalent to a value of n=1. Reinhardt [41] conducted an extensive numerical study investigating

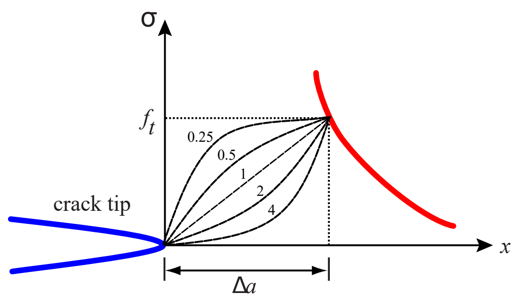

Figure 7: Non-linear stresses in fracture process zone with exponent n as a variable

the parameter n. Reinhardt's validation on normal strength concrete suggested that the value of n lies between 1.25 and 1.8. Reinhardt [41] also concluded that the stresses in the softening zone of a discrete crack comply with the assumed power function and that n increases with higher quality concrete. Therefore, a higher strength concrete would be more sensitive to cracks than a lower strength concrete.

3.3. Concrete fracture toughness (K_{Ic}) and tensile strength (f_t)

The fracture toughness, or the critical stress intensity factor, and the tensile strength of concrete significantly affect the generalised characteristic length. Test methods have been proposed to calculate both the fracture toughness and tensile strength of concrete [43].

If not measured directly in experiments, these terms can be inferred. The fracture toughness (G_F) can be calculated based on the empirical equation proposed by Phillips and Binsheng [44] where:

$$G_F = 43.2 + 1.13 f_c \tag{21}$$

where f_c is the compressive cube strength in $\mathrm{N/mm^2}$ and G_F is the fracture toughness in kN/mm. The Young's elastic modulus of concrete E can be determined from the ACI 318-05 [45] expression where:

$$E = 4.73 \left(f_{cy}\right)^{\frac{1}{2}} \tag{22}$$

where f_{cy} and E are the compressive cylinder strength in N/mm^2 and the elastic modulus in kN/mm^2, respectively. Using linear elastic fracture mechanics, the stress intensity factor (K_{IC}) can then be calculated from G_F and E:

$$K_{Ic} = \sqrt{G_F E} \tag{23}$$

f_{cy} can be calculated as 0.80% of the concrete cube strength [46] in cases where the cylinder strength is not available.

ACI 318-14 [47] suggests that:

$$f_t = 0.62\sqrt{f_{cy}} \tag{24}$$

where f_t and f_{cy} are the modulus of rupture and cylinder compressive strength in N/mm^2 respectively.

However, Carrasqillo et al [48] found that this equation underestimates the modulus of rupture strength and so have suggested that f_t can instead be found from:

$$f_t = 0.97\sqrt{f_{cy}} \tag{25}$$

where f_t and f_{cy} are the modulus of rupture and cylinder compressive strength in N/mm^2 respectively. It should be noted that the concrete material properties obtained using test methods recommended by standards are size dependent and the reader is advised to be mindful of this.

The aggregate size is not an explicit parameter in these expressions. But it has been shown that the aggregate size plays a significant role in the fracture toughness, tensile and compressive strengths of concrete [49]. Therefore, it can be deduced that the aggregate size implicitly influences the generalised characteristic length.

3.4. Crack bridging force in the reinforcement (K_{IF})

In a reinforced concrete beam subjected to bending, the internal reinforcement can carry a certain amount of force, which resists the bending. This force changes the stress field at the crack tip and the generalised characteristic length increases due to the presence of the reinforcement. If the stress intensity factor is increased, the stress distribution shifts. The characteristic length then also increases leading to a smaller size effect reduction (the value of the size effect reduction factor λ approaches 1).

Fig. 4 illustrates the force across a crack at the level of the reinforcement. When a LEFM specimen is subjected to a force across a crack, the stress intensity factor can be found (Tada et al [42]) as

$$K_{IF} = \frac{F_s}{bD^{\frac{1}{2}}} Y_F \left(\frac{a}{D}, \frac{c}{a}\right) \tag{26}$$

where F_s is the force applied across the crack, c is the cover depth (distance between the bottom fibre of the concrete beam and the centre of the reinforcement), b is the width of the beam and $Y_F\left(\frac{a}{D}, \frac{c}{D}\right)$ is the shape function for the force applied across a crack. The shape function $Y_F\left(\frac{a}{D}, \frac{c}{D}\right)$ can be given as

$$Y_F\left(\frac{a}{D}, \frac{c}{a}\right) = \sqrt{\frac{4D}{\pi a}} \frac{G\left(\frac{a}{D}, \frac{c}{a}\right)}{\left(1-\frac{a}{D}\right)^{\frac{3}{2}} \sqrt{1-\left(\frac{c}{a}\right)^2}} \tag{27}$$

where

$$G\left(\frac{a}{D}, \frac{c}{a}\right) = g_1\left(\frac{a}{D}\right) + g_2\left(\frac{a}{D}\right)\left(\frac{c}{a}\right) + g_3\left(\frac{a}{D}\right)\left(\frac{c}{a}\right)^2 + g_4\left(\frac{a}{D}\right)\left(\frac{c}{a}\right)^3 \tag{28}$$

and

$$g_1\left(\frac{a}{D}\right) = 0.46 + 3.06\left(\frac{a}{D}\right) + 0.84\left(1-\frac{a}{D}\right)^5 + 0.66\left(\frac{a}{D}\right)^2\left(1-\frac{a}{D}\right)^2 \tag{29}$$

$$g_2\left(\frac{a}{D}\right) = -3.52\left(\frac{a}{D}\right)^2 \tag{30}$$

$$\begin{aligned} g_3\left(\frac{a}{D}\right) = {} & 6.17 - 28.22\left(\frac{a}{D}\right) + 34.54\left(\frac{a}{D}\right)^2 - 14.39\left(\frac{a}{D}\right)^3 \\ & - \left(1-\frac{a}{D}\right)^{3/2} - 5.88\left(1-\frac{a}{D}\right)^5 - 2.64\left(\frac{a}{D}\right)^2\left(1-\frac{a}{D}\right)^2 \end{aligned} \tag{31}$$

$$g_4\left(\frac{a}{D}\right) = -6.63 + 25.16\left(\frac{a}{D}\right) - 31.04\left(\frac{a}{D}\right)^2 + 14.41\left(\frac{a}{D}\right)^3 - 2\left(1-\frac{a}{D}\right)^{3/2} + 5.04\left(1-\frac{a}{D}\right)^5 + 1.98\left(\frac{a}{D}\right)^2\left(1-\frac{a}{D}\right)^2 \tag{32}$$

The value of K_{IF} for a given crack depth, and the relationship between η and $\frac{a}{D}$, will also dictate whether stable or unstable crack growth is expected. It has been shown elsewhere that the forces in the reinforcement change with crack propagation and, as a consequence, K_{IF} will depend on the crack depth [50, 51, 40]. At the critical crack development stage, the force in the reinforcement is dictated by the geometry of the specimen, amount and type of reinforcement, type of concrete and bond-slip conditions between the reinforcement and concrete. In order to precisely predict the generalised characteristic length, a model is therefore required to connect the force in the reinforcement with crack depth. Models to determine the reinforcement force such as that of Carpinteri [50, 51] can be incorporated. However, the purpose of the current work is to introduce the idea of a generalised characteristic length and identify the sensitivity of the characteristic length to various parameters. So, a simplified approach where the bridging force is assumed to be a portion ($0 \leq \psi \leq 1$) of the yield force of reinforcement will be used. Introducing the factor ψ into the generalised characteristic length equation 26 leads to:

$$D_0 = \eta\frac{2n+1}{2\pi}\left(\frac{K_{Ic}}{f_t}\right)^2\left(1 + \frac{\rho D^{1/2}\psi f y Y_F\left(\frac{a}{D}, \frac{c}{a}\right)}{K_{Ic}}\right)^2 \tag{33}$$

where ρ and f_y are the percentage of longitudinal reinforcement and the longitudinal steel yield strength respectively. The reinforcement was considered to be a linear elastic plastic material.

3.5. Comparison with Bazant's and Hillerborg's characteristic lengths

For concrete beams with no reinforcement, the stress intensity factor (K_{IF}) due to the reinforcement is zero, and the generalised characteristic length reduces to an expression which depends only on the geometric and concrete material properties of the beam:

$$D_0 = \eta \frac{2n+1}{2\pi} \left(\frac{K_{Ic}}{f_t} \right)^2 \tag{34}$$

The $\left(\frac{K_{Ic}}{f_t}\right)^2$ term is the same as Hillerborg's [52] characteristic length calculated for unreinforced concrete, which is a pure material property. So for the case when $\eta \frac{2n+1}{2\pi} = 1$ and $K_{IF} = 0$, the generalised characteristic length gives an expression which is analogous to Hillerborg's result. Furthermore, K_{Ic} is believed to be a function of the aggregate size [53, 54]. Bazant and Kim [27] suggested that equivalent crack length Δa_e (Fig. 5) was approximately proportional to d_a, where d_a is the maximum aggregate size ($\Delta a_e \propto d_a$). Although it should be noted that Bazant and Kim's approximation was for a diagonal shear failure in longitudinally reinforced concrete beams, where the crack bridging effect of the steel (due to the inclination of the shear crack) was not as significant compared to reinforced concrete beams failed in bending. Furthermore, it was shown that during shear failure the longitudinal steel did not develop its full tensile capacity at the initiation of diagonal shear cracks. This proportionality factor for the characteristic length ($\Delta a_e \propto d_a$) was obtained by curve fitting with existing experimental results for longitudinally reinforced concrete beams. The generalised characteristic length presented here can be expressed as $D_0 = \eta \Delta a_e$ and so, for geometrically similar beams, the length is constant for a given Δa_e. Hence, Bazant's and Hillerborg's characteristic lengths that are based on the material properties such as the tensile strength and fracture toughness of concrete can be deduced from the proposed formulation. It should be noted that the characteristic lengths reported in the literature and generalised characteristic length derived in this paper are for a non-dimensional geometry with a specific relative crack depth. These characteristic lengths do not depend on the sample size.

4. Experimental results and reference databases

Existing studies on unreinforced and lightly reinforced beams were reviewed to extract validation data for the generalised characteristic length approach. Key criteria for inclusion in the validation databases were that the beams needed to be prismatic and failure was due to a single flexural crack in the middle of the beam. These constraints were necessary to be consistent with the theoretical derivation. It was also desirable for the beams to be geometrically similar such that η remained constant.

Experimental results for bending failures in geometrically similar unreinforced samples were collated from [12, 14, 55, 56, 57, 58, 59, 60, 61, 62, 63] and are summarised in Appendix A. In most cases, there is a single specimen for a specific size. Where more than one specimen was available, average values are reported. It should be noted that the geometry, test set-up (three- or four-point bend tests) and presence or absence of a notch differ between the tests series (for details please see Appendix A). However, for the selected results, the samples within a given series are geometrically similar.

Experimental results on size effects in longitudinally reinforced concrete beams that failed in bending were surveyed. However, for reasons discussed previously, the majority of experimental results on longitudinally reinforced concrete beams use higher percentages of reinforcement. Collectively the studies by Lepeach and Li [64] ($\rho = 1.6\%$), Belgin and Sener [22] ($\rho = 3\%$), Sreehari and Jeenu [21] ($\rho = 1.5\%$), Adachi et al [65] ($\rho = 0.72\% - 2.5\%$), Yi et al [20] ($\rho = 1.11\% - 1.33\%$), Zhou et al [66] ($\rho = 1.05\% - 1.65\%$) and Wu et al [67] ($\rho = 0.36\% - 0.44\%$) cover a range of reinforcement ratios ($0.36\% < \rho < 3\%$) and beam sizes. However in each case the authors note that the beams failed due to stable crack growth. Carpinteri et al [16, 56] ($\rho = 0.196\% - 2.01\%$), Ozbolt and Bruckner [68] (0.151%) and Ruiz et al [69] ($\rho = 0.065\% - 0.262\%$) tested beams with low percentages of reinforcement. However, Ozbolt and Bruckner's (0.151%) and Carpinteri et al's [56] (0.196%) most lightly reinforced beams were still reported to exhibit stable crack growth. In addition, Carpinteri et al's specimens were not geometrically similar. Corley et al's [19] reinforced concrete beams are not geometrically similar so η will vary between test samples. Ruiz et al's [69] ($\rho = 0.065\% - 0.262\%$) specimens were geometrically similar but the results were presented in plots (not tabulated). Hence, the relevant data that was extracted from Ruiz et al's experimental load-deformation plots is summarised in Appendix B and used in subsequent sections for further validation.

In light of the relative paucity of experimental studies on lightly reinforced geometrically similar concrete beams failing due to unstable crack growth, additional experimental testing was undertaken. The aims were to help establish the crack bridging effects in lightly reinforced concrete beams failing in bending and clarify the transition from brittle to plastic behaviour using the generalised characteristic length. Of particular interest were beams that were very lightly reinforced e.g. with $\rho < 0.1\%$.

4.1. Experimental investigation

A series of unreinforced and lightly reinforced specimens with beam depths of 50 mm, 100 mm, 150 mm and 200 mm were tested as shown in Fig. 8(a). The notch depth and the span between the support and loading plate were increased in proportion with the beam depth. However, the beam width (b) of 100 mm was the same for all the specimens. The unreinforced and reinforced cross sections are shown in Fig. 8(b) and 8(c) respectively. In the reinforced beams, the distance between the centre of the reinforcement and the bottom surface of the beam was ($0.2d$) and so varied proportionally with the beam depth to achieve geometrically similar beams. The reinforcement ratio was fixed at 0.053% and the number of bars was increased proportionally with the beam depth. To reduce any influence due to debonding, the 1.84 mm diameter bars were threaded although this is not typical of steel reinforcement used in the construction industry.

For each set of beam parameters, three specimens were prepared, and the specimens were cast from a single mix to minimise any irregularities in the concrete properties. A maximum aggregate size of 8 mm was selected to minimise

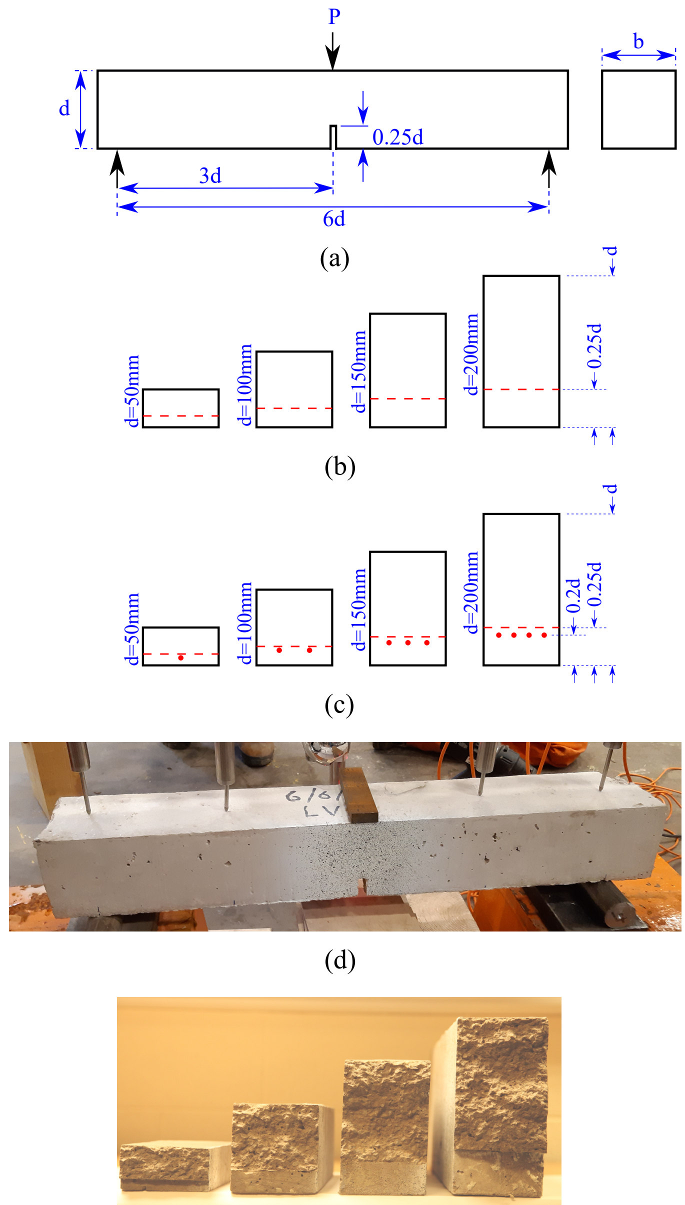

Figure 8: (a) Test set up; (b) cross sections of unreinforced beams (d=50, 100, 150, 200 mm; b=100 mm); (c) cross sections of reinforced beams (d=50, 100, 150, 200 mm; b=100 mm); (d) schematic view of test specimen and (e) cracked faces of unreinforced specimens.

Table 1: Mechanical properties of concrete and reinforcement

Concrete	
Cube strength (f_{cu})	$31.6N/mm^2$
Cylinder strength (f_{cy})	$34.8N/mm^2$
Young's modulus of elasticity (E_c)	$23800N/mm^2$
Modulus of rupture (f_t)	$4.03N/mm^2$
Fracture toughness (G_F)	$0.066N/mm$
Reinforcement	
Yield strength (f_f)	$597N/mm^2$
Young's modulus of elasticity (E_f)	$102 \times 10^3 N/mm^2$

any issues related to segregation during compaction due to the small beam size. The aggregate size was not scaled. Various concrete and steel material properties were measured using recommended test guidelines [43, 70, 71, 72]. These properties are summarised in Table 1 where each value is an average of at least three control test specimens.

The displacement at first cracking in the mid span during a displacement controlled test is expected to increase with increasing beam span. So a constant displacement rate (loading rate) is expected to lead to different kinetic forces in the samples. To minimise this effect, automated servo displacement-controlled tests were carried out with displacement rates of 1, 2, 3 and 4 mm/min for the beam depths of 50, 100, 150 and 200 mm, respectively. The beams were tested to failure and all the unreinforced and lightly reinforced beams failed due to a single flexural crack, as shown in Fig. 8(e). The relevant beam details and failure loads have been included in Appendices A and B for the unreinforced and reinforced beams respectively.

4.2. Application of generalised characteristic length approach to experimental findings

Across the results in the experimental databases, there are differences in terms of the presence or absence of a notch, the span to depth ratios, the smallest sample size and the material properties reported. To facilitate the comparison of disparate samples, common principles in the application of the generalised characteristic length approach were followed.

For unstable crack growth, the maximum load is associated with the initiation of a crack from the tip of the crack notch. Some of the beams within the validation database do not have notchs. As fracture theory only applies to flawed specimens, when there is no initial crack (flaw) then theoretically fracture mechanics would not yield a solution. Nevertheless concrete exhibits micro-cracking so it was deemed justifiable to assume a virtual crack notch of 0.2 for concrete specimens without notchs. Therefore the value of η was either calculated at the depth of crack inducer (notch depth) or at the depth of a virtual crack notch for the beams with no physical crack notch. The database span to depth ratios range from s/d=0.75 to s/d=4. The shape functions reported earlier do not cover all these cases. So the geometric shape constant η was interpolated for beams with shear span to depth ratios (s/d) less than 4, using the shape functions for $s/d = 2$ and $s/d = 4$. For example, for a shear span to depth ratio of $s/d = 3$ and relative crack notch depth of 0.25, η would be taken as 7.097 (see Fig. 6(b)). The pure bending η function was used when a specimen's shear span to depth was greater than 4.

If not tested experimentally, the material properties K_{Ic} and f_t were calculated using the approaches presented in section 3.3.

A challenge when using the characteristic length to calculate the size effect reduction is the need to define a plastic strength σ_c. In the current work, baselines based on expressions for f_t found in Equations (25) and (24), or an empirical approach were used. In the empirical approach the smallest sized beam in a given beam series is used to define the nominal plastic strength. The drawback is that the experimental beam series use different smallest sized beams

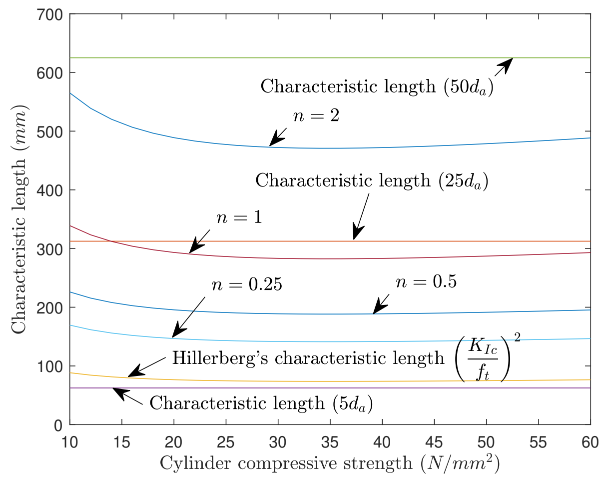

Figure 9: Comparison of generalised characteristic lengths for various values of n, Hillerborg's characteristic length and lengths of $5d_a$, $25d_a$ and $50d_a$ (with an assumed maximum aggregate size of $d_a = 12.5mm$) which are indicative of the range suggested by Bazant [73].

so the baseline beam size is then not the same when comparing different series.

5. Generalised characteristic length and size effects for unreinforced concrete

5.1. Generalised characteristic length predictions for unreinforced concrete

A theoretical study was undertaken to explore how the concrete strength and assumed concrete stress distribution influences the predicted generalised characteristic lengths for unreinforced concrete. In the theoretical predictions, a shear span to depth ratio of $s/d = 3$ and relative crack notch depth of 0.25 were assumed and hence $\eta = 7.097$. In Fig. 9, the generalised characteristic lengths using values of n of 0.25, 0.5, 1 and 2 have been plotted for different concrete compressive strengths. Hillerborg's characteristic length and characteristic lengths of $5d_a$, $25d_a$ and $50d_a$ have been included in the figure for comparison purposes.

As expected, Hillerborg's characteristic length is smaller than the generalised characteristic length prediction, even for n=0.25. As described in Section 3.5, Bazant considered that the characteristic length is proportional to the maximum aggregate size (d_a). Bazant and Kim proposed a characteristic length of $25d_a$ using a statistical curve-fitting approach on experimental results on longitudinally reinforced concrete beams that failed in shear [27]. A characteristic length of $25d_a$ is not dissimilar to that obtained using $n = 1$ as shown in Fig. 9. Later, to predict the experimental results of reinforced concrete beams with shear links, Bazant and Sun added a term, which depends on the percentage of shear links, to $25d_a$ to modify the characteristic length. In this case, the characteristic length was considered a system property [29]. Bazant's recent statistical analyses suggest that the multiplier on d_a is between 5 and 50 [73], indicative values ($5d_a$, $25d_a$ and $50d_a$) within these bounds are plotted in Fig. 9, and confirm that the generalised characteristic length is consistent with the statistical observations. However, a characteristic length that is solely a function of aggregate size is not a direct indicator of concrete strength. Reinhardt [74] showed that the value of n varies with concrete strength. So this variation could be captured in the generalised characteristic length approach where different n values could be used for different concrete strengths.

5.2. Implication of selection of nominal plastic strength and value of n

The unreinforced experimental results reported here were used to demonstrate how the selection of the value of n and the nominal plastic strength influence the expected size effect reductions.

The size reduction factor $\left(\lambda = \frac{\sigma_{Nu}}{\sigma_c}\right)$ was plotted against the non-dimensional ratio $\frac{D}{D_0}$ in a log-log graph as shown in Fig. 10. In this figure, the plastic line (the size independent flexural strength of the concrete beams as plasticity theory does not recognise size effects) is plotted and the LEFM curve represents the $\sqrt{\frac{D}{D_0}}$ size effect. Bazant's size effect Eqn. 7 is presented in Fig. 10 as a curve. σ_{Nu} is the measured experimental strength for a given beam (see Appendix A) and the circled point is the location associated with n=1 and a σ_c

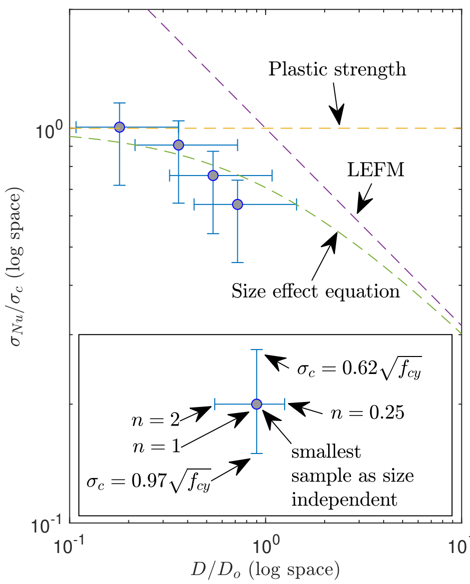

Figure 10: Sensitivities of modulus of rupture and value of n: modulus of rupture is varied between $0.62\sqrt{f_{cy}}$ and $0.97\sqrt{f_{cy}}$, which shifts the location vertically and n is varied between 0.25 and 2, which shifts the location horizontally.

determined from the failure of the smallest beam (50 mm deep). The value n=1 represents a linear stress distribution in the fracture process zone. According to Bazant's size effect law (equation 7), the strength of smaller samples approaches the plastic strength. Hence, the size effects of the larger samples were calculated by considering the smallest sample as size independent. The selected n values and size independent modulus of rupture dictate the location of the experimental results. n alters the generalised characteristic length D_0 and thus $\frac{D}{D_0}$. The horizontal bar in Fig. 10 shows the effect of a change in D_0 due to different n values where the left limit is for $n = 2$ and the right limit is for $n = 0.25$. A different reference strength shifts a point vertically where the bottom limit was based on the modulus of rupture strength calculated using Eqn. 25 and the top limit was that based on Eqn. 24.

5.3. *Unreforced size effect reduction factors and validation against experimental database*

The experimental data compiled in Appendix A was used to determine appropriate n values and to validate the generalised characteristic length predictions for unreinforced concrete. Unless stated otherwise, the size effect reduction factor (λ) was obtained using the modulus of rupture strength calculated from Eqn. 25 [48] as the baseline.

The size effect reduction factor in Eqn. 8 can be rearranged in the form of a linear regression equation ($y = mx + c$) as:

$$\frac{1}{\lambda^2} = \frac{1}{D_o} D + 1 \tag{35}$$

where $m = \frac{1}{D_o}$ and $c = 1$.

A plot of $\frac{1}{\lambda^2}$ versus the beam depth (D) for the database of unreinforced beams is shown in Fig. 11(a). In this statistical analysis, the elimination of outliers was not considered to be appropriate as there are limited experimental results available for geometrically similar beams. It should be noted that any deviations in λ, which are due to inevitable variations in the experimental results and the issue of defining the plastic strength, amplify the values in the vertical axis of Fig. 11(a) as the inverse of lambda is squared $\left(\frac{1}{\lambda^2}\right)$. When all the results were grouped together, a linear regression analysis suggested a best fit characteristic length of $D_o \approx 136$ mm. There is significant scatter in the results and the R^2 is 0.4201. However, Bazant and Planas [75] show that the size effect reduction factor differs between concrete and mortar and others suggest that the size effect reduction is significantly higher in high strength concrete [76]. For these reasons, the data gathered in Appendix A was grouped into concrete (0-50 N/mm^2), high strength concrete (HSC) (≥ 50 N/mm^2) and mortar in Fig. 11(b). Linear regression analyses were undertaken on each subcategory of data and the characteristic lengths for each subset are given in the Figure. The R^2 values for the mortar and concrete categories improved somewhat to 0.6185 and 0.5452 respectively but there was a slight reduction in the R^2 value to 0.3856

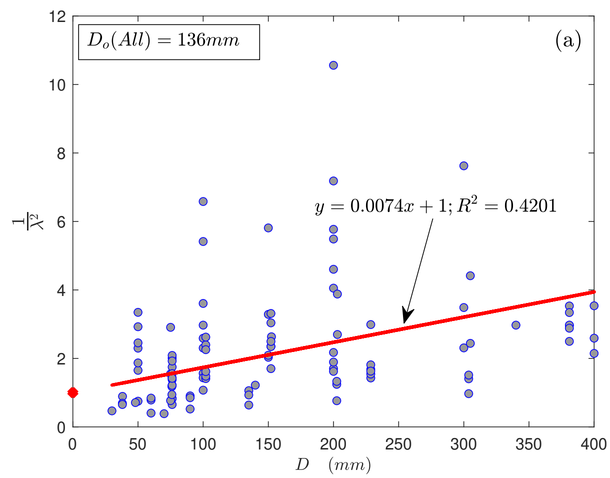

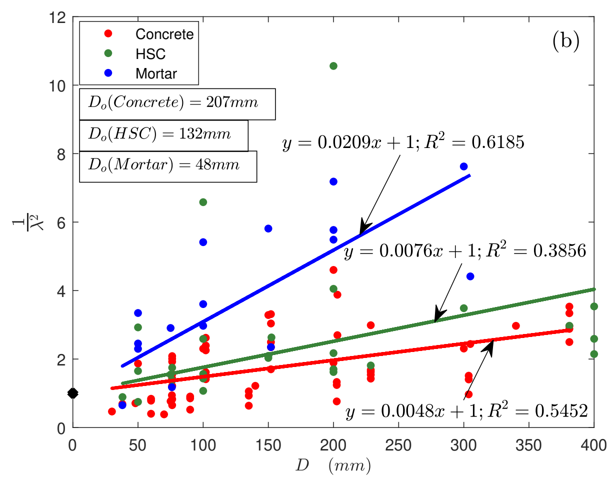

Figure 11: $\frac{1}{\lambda^2}$ vs. depth of beam D of unreinforced concrete beams presented in Appendix A (a) all the samples (b) grouped into concrete, high strength concrete (HSC) and mortar (the D_o values presented in the plots are obtained from linear regression analyses).

for the HSC. It can be seen that the best fit characteristic lengths of the HSC (132 mm) and mortar (48 mm) beams were found to be smaller than that of the normal strength concrete beams (207 mm).

Bazant contested that the aggregate size is one of the main factors that influence the size effect of concrete elements [73]. According to the generalised characteristic length, the aggregate size is an implicit parameter, which alters the mechanical properties of concrete, such as the fracture toughness and tensile strength. It can be noted that the generalised characteristic length uses the ratio between the fracture toughness and the tensile strength of concrete. To understand the impact of aggregate size on the generalised characteristic length, existing experimental results which investigate the effect of fracture toughness and tensile strength with varying aggregate sizes are discussed.

Elice and Rocco [49] tested two different concrete matrices each with three different untreated aggregates (with average sizes of 3, 9 and 14 mm). For matrix one, the fracture toughness increased by 20% whereas the tensile strength decreased by 6% when the average aggregate size increased from 3 mm to 14 mm. For matrix two, the fracture toughness increased by 16% when the aggregate size increased from 3 mm to 14 mm but there was no observable change in tensile strength. Petersson [77] showed that the fracture toughness increased by 13% while the tensile strength decreased by 12.5% when the maximum aggregate size increased from 8 mm to 16 mm. Chen and Liu [78] also showed that the fracture toughness increased with aggregate size and observed a 37% increase in toughness when the maximum aggregate size increased from 10 mm to 20 mm. However, Chen and Liu did not investigate the tensile strength. Saouma et al. [79] tested larger size aggregates and found that the fracture toughness increased by 31% while the tensile strength decreased by 7% when the maximum aggregate size increased from 19 mm to 76 mm. In Rao and Prasad's [80] work, an increase in maximum aggregate size from 4.75 mm to 20 mm led to an increase in fracture toughness of 84% and a 28% increase in tensile strength.

In general it has therefore been found that the fracture toughness increases with aggregate size. Chen and Liu [78] studied the crack surfaces using X-ray inspection and showed that the width of the crack increases with aggregate size. A narrower crack width results in a smoother crack surface, while a broader crack width results in a rough and complex crack surface and hence an increase in fracture energy with increasing aggregate size. The trends for tensile strength are more varied. Nevertheless, all the reported findings would lead to an increase in the ratio $\left(\frac{K_{Ic}}{f_t}\right)^2$ in Eqn. 34 with increasing aggregate size. So a larger aggregate size would increase the generalised characteristic length and a corresponding reduction in size effect would then be expected.

The findings in Figure 11(b) support the conclusion that for a given beam depth the size effect reductions are higher for HSC and mortar than for normal strength concrete [60, 81, 82, 76, 83]. However, it should be noted that the characteristic length is also related to the exponential power (n) of the non-linear stress distribution in the fracture process zone. Existing knowledge and understanding as to how the aggregate size influences the n value is limited. But, the generalised characteristic length allows for such differences to be accommodated through the adjustment of n.

As previously illustrated in Fig 10, the location of the experimental results (data points) are dictated by the characteristic length and the plastic strength of the sample. These dependencies are further demonstrated in Fig. 12, where the size effect reduction factor $\lambda\left(=\frac{\sigma_{Nu}}{\sigma_c}\right)$ is plotted against the ratio between the beam depth and characteristic length $\left(\frac{D}{D_o}\right)$. In Fig. 12, the horizontal line, inclined line, and curve represent the plastic strength, the LEFM and Bazant's size effect equation, respectively. The upper and lower boundaries of the shaded region are for a $\pm$ 10% variation in Bazant's size effect equation. In Fig. 12(a) and (b), a constant value of D_o of 136 mm (based on the best fit line in Fig 11(a)) is used for all the specimens in the database (Appendix A) irrespective of the material and geometric properties. In Fig 12(a) the plastic strength was taken as modulus of rupture strength whereas in Fig. 12(b) the smallest sample is taken to be size-independent; thus, the smallest sample manifests the plastic strength. The experimental data points shift vertically (no horizontal shift) when the reference plastic strength changes (Fig. 12(a) vs Fig. 12(b)) while D/Do remains the same. The scatter in Fig. 12(a) and (b) illustrates that the characteristic length is a complex material and geometric property, which cannot be deduced from a single characteristic length value. Fig. 12 (c) and (d) use Hillerberg's characteristic lengths, where the characteristic length parameter is based on pure material properties. Again, the influence of the plastic reference strength can be observed in the difference between Fig 12(c) (modulus of rupture reference strength) and Fig 12(d) (smallest size reference strength). A comparison of Fig. 12(a) vs Fig 12(c) and Fig 12(b) vs Fig 12(d) shows that the locations of the experimental data points shift horizontally (no vertical shift) due to the changes in the predicted characteristic length. Most experimental data points in Fig 12(d) lie outside the shaded size effect equation region which suggests that the characteristic length cannot be a material property alone. Fig. 12 (e) and (f) use the generalised characteristic length with a fixed value of n=1. The experimental data shifts and is more aligned in Fig 12 (f) to the size effect predictions than was the case in Fig 12(d). This suggests that the characteristic length is a function of not only the material properties but also the geometric properties (system properties). To further explore the influence of the stress distribution in the fracture process zone n is varied in Fig. 12(g) and Fig. 12(h) where the generalised characteristic length predictions used $n = 1$ for normal concrete, $n = 0.4$ for HSC and $n = 0.2$ for mortar. As previously demonstrated by Reinhardt [41, 74], the stress distribution within the fracture process zone depends on the concrete properties. The current understanding of the shape of the stress distribution within the fracture process zone, as is required to quantify n, for different concrete and mortars is limited. However, the trends shown in Fig 12(h) suggest that implementation of material specific n values could lead to improved size effect predictions. Overall, the results illustrate that the characteristic length is a system property. Moreover, the generalised characteristic length theory provides a more solid explicit understanding of how the characteristic length changes with the basic properties of concrete and the overall system.

In Fig. 12, the size effect reduction factors were calculated by assuming the plastic strength was either the modulus of rupture strength or the smallest sample strength in each subset. The results demonstrate that the modulus of rupture strength is size-dependent when obtained using recommended test standards. The depths of the smallest samples in all the test series are between 30 and 100 mm, which are smaller than the test samples recommended by standards. It is therefore felt to be reasonable to assume that the smallest sample in a given experimental series is size-independent, albeit different sample depths were taken as size-independent within each subset. This shows that the appropriate plastic strength is important to establish the size effect. Inverse methods could potentially be applied to help establish a size independent plastic strength [84].

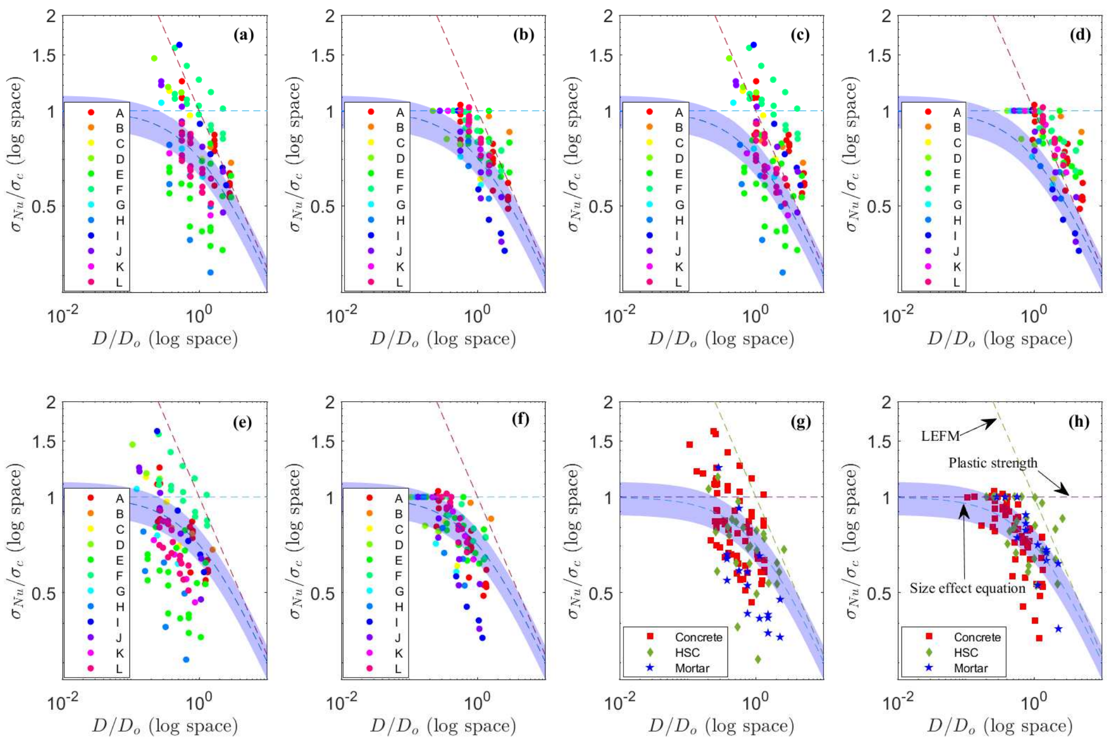

Figure 12: Size effect reductions for experimental unreinforced concrete beams: (a) $D_o = 136$ mm (See Fig. 11(a)) and $\lambda\,(=\sigma_{Nu}/\sigma_c)$ calculated assuming the plastic strength as $\sigma_c = 0.97\sqrt{f_{cy}}$; (b) $D_o = 136$ mm and λ calculated assuming the smallest beam of the subset is size-independent; (c) D_o calculated using Hillerberg's characteristic length expression $(K_{Ic}/f_t)^2$ and λ calculated assuming the plastic strength is $0.97\sqrt{f_{cy}}$; (d) D_o calculated using Hillerberg's characteristic length expression $(K_{Ic}/f_t)^2$ and λ calculated assuming the smallest beam of the subset is size-independent; (e) D_o calculated from the generalised characteristic length with $n = 1$ and λ calculated assuming the plastic strength is $0.97\sqrt{f_{cy}}$; (f) D_o calculated from the generalised characteristic length with $n = 1$ and λ calculated assuming the smallest beam of the subset is size-independent; (g) D_o calculated from the generalised characteristic length with $n = 1$ for normal strength concrete, $n = 0.4$ for HSC and $n = 0.2$ for mortar and λ calculated assuming the plastic strength is $0.97\sqrt{f_{cy}}$; and (h) D_o calculated from the generalised characteristic length with $n = 1$ for normal strength concrete, $n = 0.4$ for HSC and $n = 0.2$ for mortar and λ calculated assuming the smallest beam of the subset is size-independent. The upper and lower limits of the shaded region are 10% higher and lower than the size effect equation, respectively.

6. Lightly reinforced concrete beams

6.1. Generalised characteristic length predictions for lightly reinforced concrete

Figure 13(a) illustrates the theoretical relationship between the generalised characteristic length and the depth of lightly reinforced concrete beams with various percentages of reinforcement. For this theoretical prediction, the same geometry and material properties presented in Fig. 8 and Table 1 are used. i.e. for a concrete beam without reinforcement, a generalised characteristic length of $D_o \approx 323mm$ was calculated using Eqn. 34 with $\eta = 7.097$ which corresponds to a shear span to depth ratio of s/d=3 and relative crack notch depth of a/D=0.25 with concrete material properties $K_{Ic} = 39.63$ N/mm$^{\frac{3}{2}}$, f_t=4.03 N/mm^2 and n=1. For a concrete beam with a longitudinal reinforcement percentage of 0.1%, yield strength of steel f_y=597 N/mm^2 and relative cover depth of c/D=0.2, K_{IF} was calculated to be 28.89 N/mm$^{\frac{3}{2}}$ for a 100mm beam depth, using Eqn. 26 and 27. For this prediction, the steel was assumed to have yielded so $\psi = 1$ in Eqn. 33. And, thus a generalised characteristic length of $D_o \approx 984mm$ was calculated using Eqn. 33.

The predictions for longitudinal reinforcement percentages of 0.1%,0.2%, 0.3% and 0.4% are compared with those of an unreinforced beam (where ρ=0). A higher ρ, which is analogous to a larger crack bridging force, leads to a larger generalised characteristic length. According to Bazant's size effect equation, a larger characteristic length then corresponds to a smaller size effect reduction.

The resulting size effect reduction factor λ is plotted as a function of beam depth in Fig. 13(b). The figure shows that the crack bridging force significantly influences the anticipated reduction. Even a relatively small percentage of longitudinal reinforcement mitigates the size effects prevalent in unreinforced beams. For unreinforced beams, reductions between 34-52% would be expected for beam sizes between 300mm and 800mm. For beams with 0.1% reinforcement, the reductions would be between 11-15% for a similar size range and as the percentage of reinforcement increases above 0.2% they would be less than 6.5%.

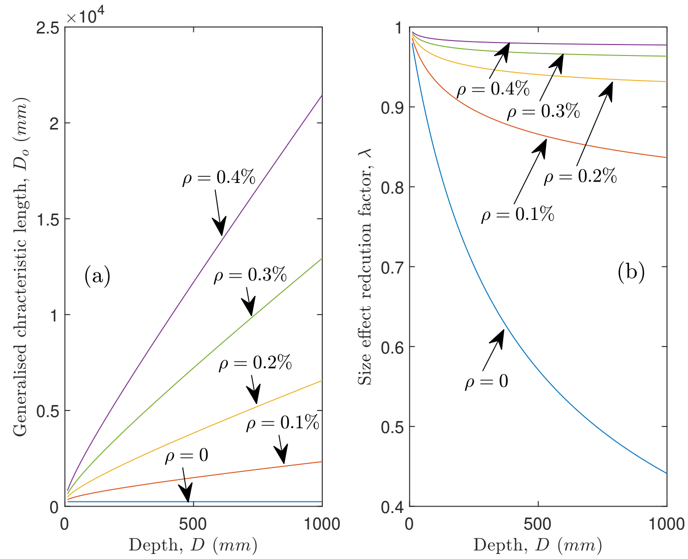

Figure 13: (a) Changes in generalised characteristic length with crack bridging force (percentage of reinforcement ratio ρ) (b) size effect reduction factor (λ)

6.2. Implication of crack bridging force

In Fig. 14, a plot of $\sigma_{Nu}/\sigma_c(= \lambda)$ versus D/D_0 using the experimental results from the current work further demonstrate the influence of the crack bridging force. The reinforcement percentage was 0.053% and the smallest sized beam (50 mm) was taken to be size-independent. The concrete was the same as that used in the companion unreinforced beams reported in Section 5.2 where n=0.35 was found to provide the best fit with the size effect equation. So n was taken as 0.35. The size effect of reinforced concrete beams is often treated solely as a concrete material property. If this were the case, the characteristic length of a reinforced concrete beam would be independent of the steel force. Fig. 14(a) illustrates the experimental results for the reinforced concrete beams, where the effect of the reinforcement is neglected by assuming $K_{IF} = 0$ in the generalised characteristic length formulation. The data points are all to the right of Bazant's size effect equation. In the generalised characteristic length theory, the characteristic length depends on the crack bridging force from the reinforcement too. However, the force exerted by the reinforcement at the critical stage of crack development has not yet been fully established. Thus, the crack bridging force was varied from zero (ψ=0) to 50% of the yield force (ψ=0.5) to the full yield force (ψ=1), as shown in Fig. 14(b). As the crack bridging force increases, the location of the experimental results shift left horizontally. This is due to the increase in generalised characteristic length. According to Fig. 14 (b), the full yield force condition (ψ=1) provides the best fit with Bazant's size effect equation.

6.3. Lightly reinforced concrete size effect reduction factors and validation against experimental database

As discussed previously, there are limited suitable lightly reinforced concrete experimental results against which the generalised characteristic length approach can be validated. The class of beams that could meet the requirements need to have low reinforcement ratios and fail due to unstable crack propagation. Similar geometric and loading conditions, shear span to effective depth ratios, concrete and reinforcement properties, reinforcement percentages, bond conditions, relative cover depths and relative crack notch depths are also desirable. Furthermore, the use of the full yield strength in Equation 33 is most likely to be justified in lightly reinforced cases (e.g. $\rho \leq 0.2\%$) where the reinforcement is well-bonded and a single flexural crack exhibits unstable crack growth that leads to failure.

The subset of results that comply with these constraints were limited to the experimental beams tested here and the beam results of Ruiz et al [69] which were inferred from the plots presented in their paper. Ruiz et al did not test geometrically similar unreinforced specimens so it was not possible to back calculate an appropriate n value specifically for their concrete. Ruiz et al use a normal strength concrete with cylinder strength of 39.5MPa so based on the findings in Fig. 12, n was taken as 1. In each case, the smallest sized experimental beam was taken to be size independent. However, as discussed

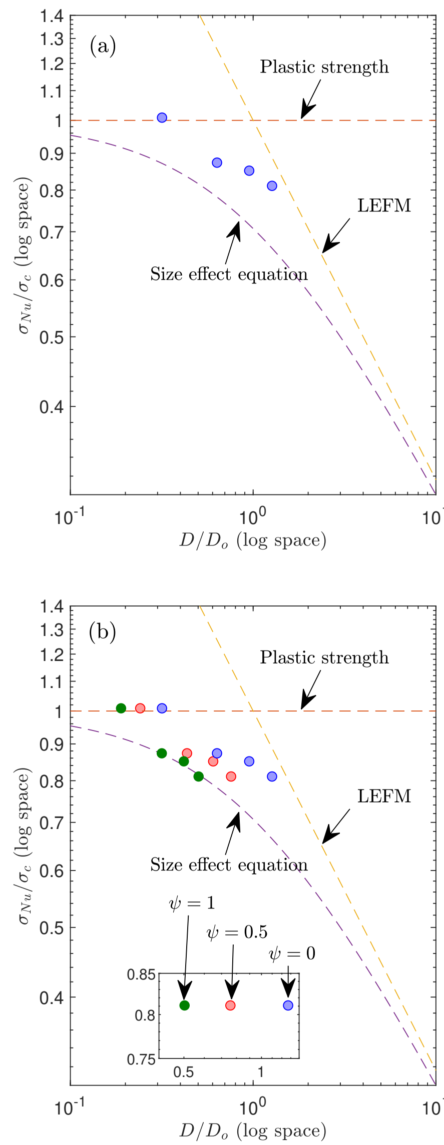

Figure 14: Current experimental reinforced concrete beams results: (a) characteristic length without crack bridging effect of reinforcement ($K_{IF} = 0$) and (b) Effect of crack bridging force in lightly reinforced experimental beams: no force ($\psi = 0$); 50% steel yield force ($\psi = 0.5$) and 100% steel yield force ($\psi = 1$) with $n = 0.35$

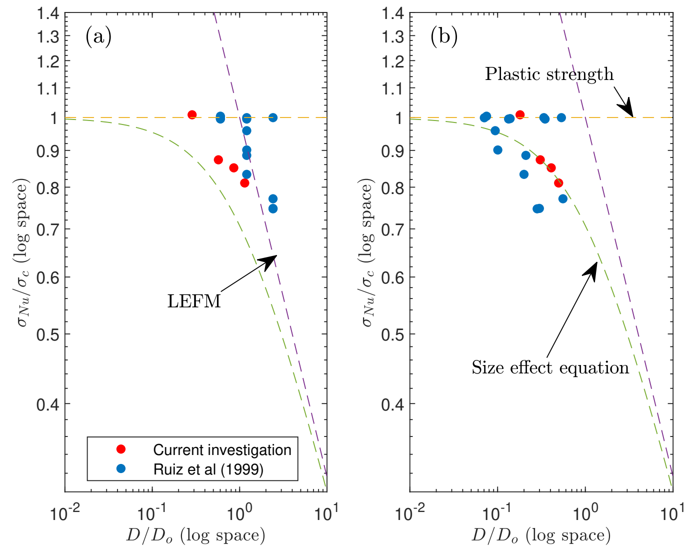

Figure 15: Current and Ruiz et al's experimental results of reinforced concrete beams as shown in appendix B: (a) D_0 was considered as materials and geometric properties with $n = 0.35$ and $n = 1$ for current investigation and Ruiz et al respectively, therefore ($K_{IF} = 0$) and (b) D_0 was calculated with full yield crack bridging force $\psi = 1$ for the corresponding percentage of steel reinforcement.

previously, if the assumption for the plastic strength is erroneous, the data points would shift vertically when plotting σ_{Nu}/σ_c versus D/D_0.

A plot of σ_{Nu}/σ_c versus D/D_0 for the selected lightly reinforced results can be found in Fig. 15. In Fig. 15(a) ψ was taken as 0 which equates to no crack bridging contribution from the reinforcement whereas in Fig. 15(b) the full yield force (ψ=1) is used.

A comparison of Fig. 15(a) and Fig 15 (b) demonstrates how the generalised characteristic length provides an explanation for the transition from brittle to ductile behaviour in the presence of reinforcement. According to the model, the generalised characteristic length significantly increases with increasing force in the reinforcement such that size effects diminish. Hence the inclusion of the crack bridging force where ψ=1 (as in Fig. 15(b)) leads to a better agreement with the size effect equation than when bridging forces are neglected (as in Fig. 15(a)). According to the size effect model and the generalised characteristic length, the brittleness of a reinforced concrete beam (unstable crack growth) and thus the size effect recedes with increasing reinforcement. Reinforced concrete elements migrate from brittle (unstable) to ductile (stable) behaviour with a higher reinforcement contribution. This observation is in agreement with recent guidelines on required minimum flexural reinforcement in reinforced concrete elements, where the percentage of minimum reinforcement varies with the size [85] [86].

7. Conclusions

A new generalised characteristic length is derived to quantify size effects in unreinforced or lightly reinforced concrete beams failing in flexure due to unstable crack propagation. The 2-D formulation explicitly reveals a dependency on the geometric shape of the beam, concrete stress distribution in the fracture process zone, concrete material properties and crack bridging force due to the reinforcement (when present). The generalised approach has certain advantages over other characteristic lengths since the unknown parameters can be derived from first principles.

Size effect predictions using the new formulation were initially validated using experimental results reported here for tests on unreinforced and lightly reinforced (0.053%) concrete beams with depths varying from 50 mm to 200 mm. The experimental unreinforced and reinforced concrete beam strengths reduced by $\approx 36\%$ and $\approx 15.5\%$ respectively when the beam depth increased from 50 mm to 200 mm. The generalised characteristic length predictions capture the experimental trends for the loss of strength with size. However, the agreement depends on the assumed reference nominal plastic strength and parameter n which describes the shape of the stress distribution in the fracture process zone.

Validation against a wider database of unreinforced concrete beams in the literature further suggests that the choice of n is influential in the generalised characteristic length predictions. There was a better correlation when beams with different concrete types were grouped into categories of normal strength concretes, high strength concretes and mortars and appropriate values of n (1, 0.4 and 0.2 respectively) were assigned to each category. The generalised characteristic predictions showed a better agreement with the size effect equation than those obtained using a single fixed characteristic length or Hillerborg's characteristic length.

In reinforced beams, the crack bridging force is required in the generalised approach. A database of very lightly reinforced beams that fail due to unstable crack propagation was therefore considered for validation purposes. While there were limited results that met the necessary criteria, the initial comparison suggests that the use of the steel yield force may be a reasonable assumption.

For concrete beams that fail in flexure due to mode I fracture, the generalised characteristic length approach offers a powerful means to demonstrate the influence of longitudinal steel on the size effect. Using the concrete properties and geometric shape reported in this study, the predicted change in flexural strength with beam depth was calculated using the generalised characteristic length theory. The analyses show that an increase in beam depth from 100 mm to 1000 mm would lead to a 43% reduction in the predicted flexural strength of an unreinforced beam. The predicted flexural strength reduction for the same increase in depth (100 mm to 1000 mm) is only 7.3% for a beam reinforced longitudinally with 0.1% steel. The flexural strength reductions decline even further to 2.2%, 0.9% and 0.5% for reinforcement ratios of 0.2%, 0.3% and 0.4%, respectively.

Acknowledgments

The first author wishes to express sincere gratitude and appreciation to the Overseas Research Studentship and the Cambridge Commonwealth Trust for financing this research work. He is also grateful for the positive discussions with Dr. Chris Morley when developing the generalised characteristic length.

References

[1] W. Weibull, A statistical theory of the strength of materials, in: Royal Swedish Academy of Engineering Sciences Proceedings, no. 151, Stockholm, Sweden, 1939, pp. 1–45.

[2] Z. Bažant, B. Oh, Crack band theory for fracture of concrete, Matériaux et construction 16 (1983) 155–177.
URL `http://link.springer.com/article/10.1007/BF02486267`

[3] Z. P. Bazant, Size effect in blunt fracture: Conrete, rock, metal, Journal of Engineering Mechanics 110 (1984) 518–535.

[4] Z. P. Bažant, M. Vořechovsky, D. Novák, Asymptotic prediction of energetic-statistical size effect from deterministic finite-element solutions, Journal of Engineering Mechanics 133 (2) (2007) 153–162. `doi:10.1061/(ASCE)0733-9399(2007)133:2(153)`.

[5] P. Bažant, Q. Yu, Universal Size Effect Law and Effect of Crack Depth on Quasi-Brittle Structure Strength, Journal of Engineering Mechanics 135 (February) (2009) 78–84. `doi:10.1061/(ASCE)0733-9399(2009)135`.

[6] C. G. Hoover, Z. P. Bazant, Universal Size-Shape Effect Law Based on Comprehensive Concrete Fracture Tests, Journal of Engineering Mechanics 140 (March) (2014) 473–479. `doi:10.1061/(ASCE)EM.1943-7889.0000627`.

[7] H. W. Reinhardt, Xu S., Crack extension resistance based on the cohesive force in concrete, Engineering Fracture Mechanics 64 (1999) 563–587.

[8] J. F. Unger, S. Eckardt, Multiscale Modeling of Concrete, Archives of Computational Methods in Engineering 18 (3) (2011) 341–393. `doi:10.1007/s11831-011-9063-8`.

[9] D.-c. Feng, J.-y. Wu, Phase- field regularized cohesive zone model (CZM) and size e ff ect of concrete, Engineering Fracture Mechanics 197 (April) (2018) 66–79. `doi:10.1016/j.engfracmech.2018.04.038`.

[10] V. Mechtcherine, A. Gram, K. Krenzer, J.-H. Schwabe, S. Shyshko, N. Roussel, Simulation of fresh concrete flow using Discrete Element Method (DEM): theory and applications, Materials and Structures 47 (2014) 615–630. doi:10.1617/s11527-013-0084-7.

[11] P. Grassl, D. Grégoire, L. Rojas, G. Pijaudier-cabot, International Journal of Solids and Structures Meso-scale modelling of the size effect on the fracture process zone of concrete, International Journal of Solids and Structures 49 (13) (2012) 1818–1827. doi:10.1016/j.ijsolstr.2012.03.023.
URL http://dx.doi.org/10.1016/j.ijsolstr.2012.03.023

[12] P. F. Walsh, Fracture of plain concrete, The Indian Concrete Journal 46 (11) (1972) 469–470.

[13] P. F. Walsh, Crack initiation in Plain concrete, Magazine of Concrete Research 28 (94) (1976) 37–41.

[14] Z. Bazant, P. Pfeiffer, Determination of fracture energy from size effect and brittleness number, ACI Materials Journal 84 (November-December) (1987) 463–480.
URL http://www.concrete.org/Publications/ACIMaterialsJournal/ACIJournalSearch.aspx?m=details&ID=2526

[15] G. Ruiz, J. Planas, M. Elices, Cuantia minima en flexion: Teoria y normative, Anales de Mechnica de la Fractura 13 (1996) 386–391.

[16] A. Carpinteri, Energy dissipation in R.C. Beams under cyclic loadings, Engineering Fracture Mechanics 39 (2) (1991) 177–184.

[17] W. H. Gerstle, P. D. Partha, N. N. V. Prasad, P. Rahulkumar, Xie M., Crack growth in flexural members - a fracture mechanics approach, ACI Structural Journal 89 (6) (1992) 617–625.

[18] A. Hillerborg, Fracture mechanics concepts applied to moment capacity and rotational capacity of reinforced concrete beams, Engineering Fracture Mechanics 35 (1-3) (1990) 233–240. doi:10.1016/0013-7944(90)90201-Q.

URL http://www.sciencedirect.com/science/article/pii/001379449090201Q

[19] Corley G. W., Rotational capacity of reinforced concrete beams, ASCE Proceedings 92 (5) (1966) 121–146.

[20] S. T. Yi, M. S. Kim, J. K. Kim, J. H. J. Kim, Effect of specimen size on flexural compressive strength of reinforced concrete members, Cement and Concrete Composites 29 (3) (2007) 230–240. doi:10.1016/j.cemconcomp.2006.11.005.

[21] S. Sreedhari, G. Jeenu, Size Effect on Flexural Behaviour of Reinforced High Strength Concrete Beams, International Journal of Engineering and Technical Research (IJETR) 2 (9) (2014) 221–226.

[22] Ç. M. Belgin, S. Şener, Size effect on failure of overreinforced concrete beams, Engineering Fracture Mechanics 75 (8) (2008) 2308–2319. doi:10.1016/j.engfracmech.2007.09.006.

[23] E. Syroka-Korol, J. Tejchman, Experimental investigations of size effect in reinforced concrete beams failing by shear, Engineering Structures 58 (2014) 63–78.

[24] G. Kani, The riddle of shear failure and its solution, ACI Journal Proceedings 61 (April) (1964) 441–467.
URL http://www.concrete.org/Publications/ACIMaterialsJournal/ACIJournalSearch.aspx?m=details&ID=7791

[25] G. Kani, How safe are our large reinforced concrete beams?, ACI journal proceedings 64 (March) (1967) 128–141.
URL http://www.concrete.org/Publications/ACIMaterialsJournal/ACIJournalSearch.aspx?m=details&ID=7549

[26] E. Bentz, S. Buckley, Repeating a classic set of experiments on size effect in shear of members without stirrups, ACI structural journal 102 (November-December) (2005) 832–838.

URL http://www.concrete.org/Publications/ACIMaterialsJournal/ACIJournalSearch.aspx?m=details&ID=14791

[27] Z. P. Bazant, Kim J. K., Size effect in shear failure of longitudinally reinforced beams, Journal of the American Concrete Institute 81 (5) (1984) 456–468.

[28] P. J. Gustafsson, Hillerborg A., Sensitivity in shear strength of longitudinally reinforced concrete beams to fracture energy of concrete, ACI Structural Journal 85 (3) (1988) 286–294.

[29] Z. Bazant, H. Sun, Size effect in diagonal shear failure: influence of aggregate size and stirrups, ACI Materials Journal 84 (July-August) (1987) 259–272.

[30] G. R. Irwin, Fracture, in: In handbuch der Physik, Vol. 6, Flugge, ed., Springer-Verlag, Berlin, 1958, pp. 551–590.

[31] G. R. Irwin, Analysis of stresses and strains near end of a crack traversing a plate, Journal of Applied Mechanics 24 (3) (1957) 361–364.

[32] G. A. Plizzari, LEFM applications to concrete gravity dams, Journal of engineering mechanics 123 (8) (1997) 808–815.

[33] K. So, B. Karihaloo, Shear Capacity of Longitudinally Reinforced Beams–A Fracture Mechanics Approach, ACI structural Journal 90 (November-December) (1993) 591–600.
URL http://www.concrete.org/Publications/ACIMaterialsJournal/ACIJournalSearch.aspx?m=details&ID=4489

[34] Y. S. Jeng, Shah S. P., Nonlinear fracture parameters for cement based composites: Theory and experiments, in: NATO ASI Series, Series E: Applied Sciences, no. 94, 1985, pp. 319–359.

[35] P. Nallathambi, Karihaloo B. L., Determination of specimen-size independent fracture toughness of plain concrete, Magazine of Concrete Research 38 (135) (1986) 67–76.

[36] M. Elices, J. Planas, The equivalent elastic crack: 1. Load-Y equivalences, International Journal of Fracture 61 (2) (1993) 159–172. doi:10.1007/BF00012455.

[37] ACI Committee 318, Building code requirements for structural concrete (ACI 318–19), Tech. rep., American Concrete Institute, Farmington Hills, MI (2019).

[38] EN-1992-1-1:2004, EUROCODE 2: DESIGN OF CONCRETE STRUCTURES-PART 1-1: GENERAL RULES AND RULES FOR BUILDINGS, Tech. rep., British Standard Institution, London, UK (2005).

[39] A. Carpinteri, G. Lacidogna, N. Pugno, Structural damage diagnosis and life-time assessment by acoustic emission monitoring, Engineering Fracture Mechanics 74 (2007) 273–289. doi:10.1016/j.engfracmech.2006.01.036.

[40] C. Bosco, A. Carpinteri, Fracture behaviour of beam cracked across reinforcement, Theoretical and Applied Fracture Mechanics 17 (1992) 61–69.

[41] H. W. Reinhardt, Fracture mechanics of fictitious crack propagation in concrete, Heron 29 (2) (1984) 3–42.

[42] H. Tada, P. C. Paris, G. R. Irwin, The stress analysis of cracks handbook, Tech. rep., Del Research Corporation, Hellertown, PA. (1985).

[43] RILEM, Determination of the fracture energy of mortar and concrete by means of three-point bend tests on notched beams, Materials and Structures 18 (4) (1985) 287–290. doi:10.1007/BF02472918.
URL http://www.springerlink.com/index/10.1007/BF02472918

[44] D. V. Phillips, Binsheng Z., Direct tension tests on notched and un-notched plain concrete specimens, Magazine of Concrete Research 45 (162) (1993) 25–35.

[45] A. C. I. Committee, Building code requirements for structural concrete (ACI 318-05) and commentary (ACI 318R-05), American Concrete Institute, 2005.

[46] F. K. Kong, R. H. Evans, Reinforced and prestressed concrete,, 3rd Edition, Chapman and Hall, London, 1987.

[47] ACI Committee 318, Building Code Requirements for Structural Concrete (ACI 318-14)[and] Commentary on Building Code Requirements for Structural Concrete (ACI 318R-14), 2014.

[48] R. L. Carrasquillo, A. H. Nilson, F. O. Slate, Properties of High Strength Concrete Subjectto Short-Term Loads, in: ACI Journal ProceedingsJournal Proceedings, Vol. 78, 1981, pp. 171–178.

[49] M. Elices, C. G. Rocco, Effect of aggregate size on the fracture and mechanical properties of a simple concrete, Engineering Fracture Mechanics 75 (13) (2008) 3839–3851. doi:10.1016/j.engfracmech.2008.02.011.

[50] A. Carpinteri, A fracture mechanics model for reinforced concrete collapse, in: Proceedings of the IABSE Colloquium on Advanced Mechanics of Reinforced Concrete, 1981, pp. 17–30.

[51] A. Carpinteri, Stability of fracturing process in RC beams, Journal of Structural Engineering 110 (3) (1984) 544–558.

[52] A. Hillerborg, Theoretical basis of a method to determine the fracture energy GF of concrete, Materials and Structures 106 (1985) 291–296.

[53] Z. P. Bazant, Becq-Giraudon E., Statistical prediction of fracture parameters of concrete and implications for choice of testing standard, Cement and Concrete Research 32 (4) (2002) 529–556.

[54] CEB-FIP, Model code for concrete structures, Tech. rep., Lausanne, Switzerland (1990).

[55] C. Bosco, A. Carpinteri, P. G. Debernardi, Minimum Reinforcement in High-Strength Concrete, Journal of Structural Engineering 116 (2) (1990) 427–437. doi:10.1061/(ASCE)0733-9445(1990)116:2(427). URL http://ascelibrary.org/doi/10.1061/%28ASCE%290733-9445%281990%29116%3A2%28427%29

[56] C. Bosco, A. Carpinteri, P. Debernardi, Fracture of reinforced concrete: scale effects and snap-back instability, Engineering Fracture Mechanics 35 (415) (1990) 665–677.

[57] G. A. Rao, B. K. R. Prasad, Size effect in structural high strength concrete, in: International Association of Fracture Mechanics for Concrete and Concrete Structures, Vail, USA, 2004.

[58] B. Karihaloo, H. Abdalla, Q. Xiao, Size effect in concrete beams, Engineering Fracture Mechanics 70 (7-8) (2003) 979–993. doi:10.1016/S0013-7944(02)00161-3.

[59] T. Muralidhara Rao, T. D. Gunneswara Rao, Size Effect of Plain Concrete Beam- An Experimental Study, International Journal of Research in Engineering and Technology 02 (06) (2013) 1047–1055. doi:10.15623/ijret.2013.0206023. URL https://ijret.org/volumes/2013v02/i06/IJRET20130206023.pdf

[60] R. Gettu, Z. P. Bazant, M. E. Karr, Fracture properties and brittleness of high-strength concrete, ACI Materials Journal 87 (6) (1990) 608–618. doi:10.14359/2513.

[61] F. Zhou, R. Balendran, A. Jeary, Size effect on flexural, splitting tensile, and torsional strengths of high-strength concrete, Cement and Concrete Research 28 (12) (1998) 1725–1736. doi:10.1016/S0008-8846(98)00157-4. URL http://linkinghub.elsevier.com/retrieve/pii/S0008884698001574

[62] J. Xu, X. He, Size effect on the strength member, Engineering Fracture Mechanics 35 (415) (1990) 687–695.

[63] P. J. F. Wright, F. Garwood, The effect of the method of test on the flexural strength of concrete, Magazine of Concrete Research 4 (11) (1952) 67–76. doi:10.1680/macr.1952.4.11.67.
URL http://www.icevirtuallibrary.com/doi/10.1680/macr.1952.4.11.67

[64] M. Lepech, V. C. Li, Size effect in ECC structural members in flexure, in: FRAMCOS-5, Fracture Mechanics of Concrete Structures, 2004, pp. 1059–1066.

[65] H. Adachi, N. Shirai, M. Nakanishi, K. Ogino, Size effect on strength and deformation of RC beams failing in flexure, Fracture Mechanics of Concrete Structures, Proceedings of FRAMCOS-2, AEDIFICATIO Publishers, Freiburg (1995) 655–664.

[66] H. Y. Zhou, Z. B. Li, E. W. Guo, L. F. Liu, Test Study on Size Effect of Flexural Capacity of RC Cantilever Beams, Advanced Materials Research 446-449 (2012) 3160–3164. doi:10.4028/www.scientific.net/AMR.446-449.3160.
URL https://www.scientific.net/AMR.446-449.3160

[67] C. H. Wu, Y. C. Kan, C. H. Huang, T. Yen, L. H. Chen, Flexural behavior and size effect of full scale reinforced lightweight concrete beam, Journal of Marine Science and Technology 19 (2) (2011) 132–140.

[68] J. Ozbolt, M. Bruckner, Minimum reinforcement requirement for RC beams, in: European Structural Integrity Society, Vol. 24, Elsevier, 1999, pp. 181–201.

[69] G. Ruiz, M. Elices, J. Planas, Size effect and bond-slip dependence of lightly reinforced concrete beams, in: European Structural Integrity Society, Vol. 24, 1999, pp. 67–97. doi:10.1016/S1566-1369(99)80062-4.

[70] B. S. EN12390-3:2009, Testing hardened concrete: Compressive strength of test specimens, in: BS EN12390-3:2009, London, 2009.

[71] B. S. EN12390-4:2000, Testing Hardened Concrete–Part 4: Compressive Strength. Specification for Testing Machines (2000).

[72] B. S. EN12390-5:2009, 12390-3: 2009, Testing hardened concrete. Compressive strength of test specimens (2009) 12390–12395.

[73] Z. P. Bažant, Scaling theory for quasibrittle structural failure, Proceedings of the National Academy of Sciences of the United States of America 101 (37) (2004) 13400–13407. doi:10.1073/pnas.0404096101.

[74] H. Reinhardt, Crack softening zone in plain concrete under static loading, Cement and Concrete Research 15 (c) (1985) 42–52.

[75] Z. P. Bazant, J. Planas, Fracture and Size Effect in Concrete and Other Quasibrittle Materials, 1997. doi:084938284x.

[76] J. R. del Viso, J. R. Carmona, G. Ruiz, Shape and size effects on the compressive strength of high-strength concrete, Cement and Concrete Research 38 (3) (2008) 386–395. arXiv:arXiv:1011.1669v3, doi:10.1016/j.cemconres.2007.09.020.

[77] P. E. Petersson, Fracture energy of concrete: practical performance and experimental results, Cement and Concrete research 10 (1) (1980) 91–101.

[78] B. Chen, J. Liu, Effect of aggregate on the fracture behavior of high strength concrete, Construction and Building Materials 18 (8) (2004) 585–590. doi:10.1016/j.conbuildmat.2004.04.013.

[79] V. E. Saouma, J. J. Broz, E. Brühwiler, H. L. Boggs, Effect of aggregate and specimen size on fracture properties of dam concrete, Journal of Materials in Civil Engineering 3 (3) (1991) 204–218.

[80] G. A. Rao, B. K. R. Prasad, Fracture energy and softening behavior of high-strength concrete, Cement and Concrete Research 32 (2) (2002) 247–252.

[81] Z. Bazant, W. F. Schell, Fatigue fracture of high-strength concrete and size effect (1993). `doi:10.14359/3880`.

[82] F. P. Zhou, R. V. Balendran, A. P. Jeary, Size effect on flexural, splitting tensile, and torsional strengths of high-strength concrete, Cement and Concrete Research 28 (12) (1998) 1725–1736.

[83] S. Wang, M.-H. Zhang, S. T. Quek, Effect of specimen size on static strength and dynamic increase factor of high-strength concrete from SHPB test, Journal of testing and evaluation 39 (5) (2011) 898–907.

[84] K. Haidar, G. Pijaudier-Cabot, J. F. Dubé, A. Loukili, Correlation between the internal length, the fracture process zone and size effect in model materials, Materials and Structures/Materiaux et Constructions 38 (276) (2005) 201–210. `doi:10.1617/14053`.

[85] A. Carpinteri, M. Corrado, Upper and lower bounds for structural design of RC members with ductile response, Engineering Structures 33 (12) (2011) 3432–3441. `doi:10.1016/j.engstruct.2011.07.007`.
URL `http://dx.doi.org/10.1016/j.engstruct.2011.07.007`

[86] S. Sritharan, H. Wibowo, M. j. Rosentahl, J. N. Eull, J. Holombo, LRFD Minimum Flexural reinforcement Requirements, Tech. Rep. 20, Washington, DC (2019). `doi:10.17226/25527`.